ELSEVIER

Contents lists available at ScienceDirect

Soil Biology and Biochemistry

journal homepage: www.elsevier.com/locate/soilbio





Rotational diversity shapes the bacterial and archaeal communities and confers positive plant-soil feedback in winter wheat rotations

Nikolaos Kaloterakis ^{a,*} ^o, Adriana Giongo ^{b,c}, Andrea Braun-Kiewnick ^b ^o, Mehdi Rashtbari ^d, Priscilla Zamberlan ^b ^o, Bahar S. Razavi ^d, Kornelia Smalla ^b, Rüdiger Reichel ^a ^o, Nicolas Brüggemann ^a ^o

- ^a Institute of Bio- and Geosciences, Agrosphere (IBG-3), Forschungszentrum Jülich GmbH, 52428, Jülich, Germany
- b Institute for Epidemiology and Pathogen Diagnostics, Julius Kühn Institute (JKI) Federal Research Centre for Cultivated Plants, 38104, Braunschweig, Germany
- ^c Leibniz Institute of Vegetable and Ornamental Crops (IGZ), Theodor-Echtermeyer-Weg 1, 14979, Großbeeren, Germany
- d Department of Soil and Plant Microbiome, Institute of Phytopathology, Christian-Albrechts-University of Kiel, 24118, Kiel, Germany

ARTICLEINFO

Keywords: Archaea Bacteria Enzymes Microbiome Monocropping Nitrogen Rhizosphere Soil legacy Wheat

ABSTRACT

Plant-soil feedbacks drive productivity in winter wheat (WW; Triticum aestivum L.) rotations. Although this is a frequent observation, the underlying plant-soil-microbe interactions remain unclear. We aimed to investigate the effects of WW rotational positions on soil bacterial and archaeal communities, as well as nitrogen (N) cycling, as potential drivers of WW yield decline in successively-grown WW. WW following oilseed rape (W1; Brassica napus L.) was compared with WW in self-succession (W2) in a rhizotron study using agricultural soil with a sandy loam texture. Samples were collected at tillering and grain ripening. At tillering, we found a higher NO₃ content in W1 soil, especially in the 60-100 cm subsoil layer, associated with the N-rich residues of the preceding oilseed rape crop, while this trend was reversed at grain ripening. Analysis of enzyme kinetics revealed an increase in leucine aminopeptidase activity in W1 and an increase in β -glucosidase activity in W2 at tillering, possibly related to the residue quality of the preceding crop. No differences in bacterial and archaeal alpha diversity were observed at both sampling times, but beta diversity showed a significant role of both rotational position and soil depth in shaping the microbial community. The gene copy numbers of amoA genes of ammonia-oxidizing bacteria (AOB), nifH and nirS were significantly higher in W2 compared to W1 at tillering, suggesting a strong effect of rotational position on N cycling of the following WW. The abundances of amoA (AOB) and nirS were also higher in W2 at grain ripening. Our results highlight the persistent soil legacy of the preceding crop on both nutrient cycling and bacterial and archaeal community composition, contributing to yield reduction in successively grown WW. Understanding plant-microbe interactions and keeping them at the center of productive WW rotations is, and will continue to be, critical to future agriculture.

1. Introduction

Winter wheat (WW) is the second most cultivated cereal in the world, grown on approximately 217 million hectares in 2018 and providing one-fifth of the world's caloric and protein demand (Shewry and Hey, 2015; Erenstein et al., 2022). Following a linear increase of 35% since 1994, the yield growth of WW is currently stagnating, not meeting the forecasted global demand (Moore and Lobell, 2015; Schauberger et al., 2018; Erenstein et al., 2022).

It is estimated that up to 40% of the global WW is cultivated in monocropping systems (Angus et al., 2015; Yin et al., 2022). This

self-succession of WW is associated with yield reduction, mainly attributed to the fungal root pathogen *Gaeumannomyces tritici* (Gt; Palma-Guerrero et al., 2021). However, yield decline has also been observed in years lacking evident Gt infestation (Arnhold et al., 2023a, 2023b). This suggests that the yield decline in successive WW rotations is more complex, not limited to a single factor.

Temporal crop diversification by implementing suitable crop rotations holds great potential for addressing part of the WW yield decline problem. This can occur by either mitigating the negative plant-soil feedback (PSF) caused by the suppression of soil pathogens, or by conferring positive PSF, such as selecting beneficial microbes in the

E-mail addresses: n.kaloterakis@fz-juelich.de, nikoskaloter@gmail.com (N. Kaloterakis).

^{*} Corresponding author.

rhizosphere or increasing the enzymatic activity and nutrient availability. Increasing crop rotation diversity has also been associated with higher microbial activity and/or a higher incidence of plant-beneficial taxa (D'Acunto et al., 2018; Sun et al., 2023; Giongo et al., 2024). The addition of oilseed rape in the rotation as a preceding crop of WW is considered beneficial for attaining higher yields compared to less diverse crop rotations (Groeneveld et al., 2024). The positive soil legacy of oilseed rape includes suppression of pathogens through the production of secondary metabolites with biocidal properties or by simply breaking the pathogen life cycle in the soil (survival on host plant/straw residues), improving aggregate formation and soil structure, and increasing post-harvest residual nitrogen (N; Sieling et al., 2005; Weiser et al., 2017; Hegewald et al., 2018; Hansen et al., 2019; Kerdraon et al., 2019).

The positive legacy of oilseed rape can be expected to strongly affect the growth of the plants that, in turn, become more efficient in exploring the soil volume and utilizing the available nutrients in the top and subsoil. Root adaptations are strong indicators of soil resource acquisition and are controlled by both the genotype and the growing conditions of plants (Liu et al., 2022). Previous research on WW rotations has shown that factors affecting soil mineral N availability strongly affect root plasticity, at least during the early growth stages of WW (Kaloterakis et al., 2024b), which could potentially enhance nutrient and water uptake in more diverse WW rotations (Giongo et al., 2024).

Changes in the soil, and especially in the plant's rhizobiome, might reveal important information and enhance our understanding of PSFs in plant successions. The rhizosphere (RH), the interface between plants and soil microbiota, is characterized by intense microbial activity due to plant secretion of large amounts of photosynthesized carbon (C), either by exudation of low-molecular-weight compounds or of mucilage (Sasse et al., 2018). Together with the decomposing senesced roots, the rhizodeposited C stimulates microbial growth and activity in the rhizosphere, promotes nutrient cycling, and acts as a signal to recruit the rhizospheric microbial community (Benizri et al., 2007; Yuan et al., 2018; Koprivova and Kopriva, 2022; George et al., 2024). The RH is governed mainly by copiotrophic r-strategists that provide different soil functions (such as C and N cycling; Ling et al., 2022). The secretion of secondary metabolites, such as benzoxazinoids, in the RH of WW following oilseed rape is known to induce microbial community composition changes to recruit beneficial microbes to cope with pathogens, which could potentially lead to a growth tradeoff of the following WW (Hu et al., 2018; Mwendwa et al., 2021). A potential dysbiosis in the rhizosphere of monocultures, involving the depletion of keystone species that protect plants from root pathogens, reduces the disease suppressiveness of the soil compared to crop rotations (Zhou et al., 2023). In addition, plants respond by fine-tuning their rhizospheric microbial communities under N-limiting conditions (Alegria Terrazas et al., 2022). Crop rotation is an important driver of N-related gene expression (Liu et al., 2023). Despite its importance, a deeper look into the effect of WW rotational position on the diversity, composition, and activity or function of the soil bacterial and archaeal community is currently lacking, especially with respect to N cycling.

To investigate the complex processes and plant-soil interactions, we conducted a greenhouse rhizotron experiment contrasting two WW rotational positions, i.e., WW after oilseed rape (W1) and WW grown successively for two years (W2). Our research questions were: i) how does the rotational position of WW affect the soil microbial activity and specifically the activity of C and N acquiring enzymes, and consequently WW growth and productivity; and ii) how does the rotational position of WW affect the abundance of the bacteria and archaea and N-related genes. We hypothesized that the rotational position of WW would affect the bacterial and archaeal community, leading to distinct changes in the bacterial and archaeal community composition. Soil microbial activity would be affected by the WW rotational position, resulting in differences in N cycling and uptake by the following WW, and ultimately influence crop growth and yield.

2. Methods

2.1. Experimental design

The soil was collected in September 2020 from the topsoil (0–30 cm) and subsoil (30-50 cm) of field plots immediately after oilseed rape cultivation and after one year of WW cultivation following oilseed rape at the Experimental Farm Hohenschulen, Faculty of Agricultural and Nutritional Sciences, Christian-Albrechts University of Kiel (54°19′05″N, 9°58'38"E), Germany. Hereafter, they are referred to as WW rotational positions. The plots from which the soil was collected were optimally fertilized with nitrogen (240 kg N ha⁻¹) and sown with the WW cultivar "Nordkap" (SAATEN-UNION GmbH, Isernhagen, Germany). The residues of the preceding crop, i.e., oilseed rape and WW for W1 and W2, respectively, were not removed from the soil, and the field was not ploughed before soil collection. The soil is classified as a carbonate-free Cambic Luvisol of a sandy loam texture (44% sand, 35% silt, and 21% clay; Sieling et al., 2005). A detailed description of the soil properties and a comparison of the initial soil biochemical properties of this experiment is reported in Kaloterakis et al. (2024a). The residual soil nitrate (NO₃), plant available phosphorus (P), potassium (K), dissolved organic carbon (DOC) and microbial biomass C and N following oilseed rape cultivation were significantly higher than following winter wheat (Kaloterakis et al., 2024a).

Eight rhizotrons were placed in the greenhouse (Forschungszentrum Jülich, Germany). One plant was grown in each rhizotron filled with soil that had been cultivated either with oilseed rape or WW for one year before the start of the experiment (hereafter called W1 and W2, respectively). Each rotational position was replicated four times (n = 8). All rhizotrons were kept inclined at 45° to facilitate root growth along the lower side of the rhizotrons. The soil was sieved to 2 mm and, subsequently, packed into the rhizotrons to reach a bulk density of 1.45 g cm⁻³. Deionized water was added to adjust soil moisture to 70% water-holding capacity (WHC, 215 g H₂O soil kg⁻¹) at the onset of the experiment. After that, soil moisture was monitored gravimetrically and kept at 70% WHC with deionized water to ensure well-watered conditions. WW seeds from the cv. "Nordkap" were germinated in Petri dishes on sterile filter paper for 24 h in the dark at 20 $^{\circ}$ C. After germination, one seedling was planted in each rhizotron. Each plant was fertilized with 0.78 g of calcium ammonium nitrate fertilizer (13.5% NO₃-N, 13.5 NH₄-N, 4% CaO, 1% Mn, YaraBela® CAN™, YARA GmbH & Co. KG, Dülmen, Germany) corresponding to an application rate of 240 kg N ha⁻¹. It was applied in three doses of 80 kg N ha⁻¹ N ha each at the plant developmental stage BBCH (Biologische Bundesanstalt, Bundessortenamt und CHemical Industry decimal code system; Zadoks et al., 1974) 25, 30-/31 and 50, corresponding to 38, 62 and 96 days after sowing (DAS) in our experiment.

2.2. Soil sampling at tillering

The non-destructive soil sampling was performed at BBCH 29 (28 DAS; tillering, hereafter called T1). The sampling was performed as described in Reichel et al. (2022) with minor modifications. We sampled soil from two soil compartments i.e., RH and root-affected (RA) soil. For mineral N determination, we sampled soil from three soil layers i.e., 0-30 cm, 30-60 cm and 60-100 cm of four plant replicates (n = 48). Due to limitations in the maximum number of samples that could be quantified for microbiome and enzymatic analyses, we sampled soil from two soil layers i.e., 0-30 cm and 30-60 cm of three plant replicates (n = 24). Briefly, we sampled the RH soil near well-developed first-order lateral roots using a custom-made punching tool with which a hole was punched into the self-adhesive foil of the rhizotrons. Next, a soil core was extracted (2.5 cm length \times Ø 0.8 cm) by inserting an Ø 0.8 cm metal cylinder through the perforated holes of the rhizotron's plates. For the RH soil samples, the first cm of the soil core was kept for the analysis, corresponding to a volume of 0.5 cm³. We also sampled RA from holes

with no apparent root growth, but which was likely affected by the dense root system that was only partly visible on the transparent plate of the rhizotron. After soil sampling, a polyamide screw (length of 6.5 cm \times Ø 0.8 cm) resealed the hole created by the metal cylinder. To reduce soil heterogeneity in our samples, we pooled five soil sub-samples to form a composite sample at each soil compartment and soil depth. Soil samples for enzymatic analyses were stored at 4 $^{\circ}\text{C}$ and all other samples were stored at -20 $^{\circ}\text{C}$ until further processing. A preliminary analysis revealed no significant differences in the response variables (mentioned in the following subparagraphs) between RH and RA. Therefore, we combined the two soil compartments in specific analyses, which are detailed below, to increase the statistical power of our planned analyses.

2.3. Soil sampling at grain ripening and plant harvest

At the grain ripening stage (180 DAS; BBCH 90; hereafter called T2), the plants were harvested by splitting the aerial plant parts into tillers, leaves, husks, and grains. By removing the lower plate of the rhizotrons, the roots growing along the surface of the soil were exposed, and the soil profile was divided into the same soil layers described before. Since roots occupied the entire soil volume at this growth stage, we considered all the soil RH and did not distinguish between RA and RH. For mineral N determination, we sampled soil from three soil layers i.e., 0-10 cm, 10-20 cm, 20-40 cm, 40-70 cm and 70-100 cm of four plant replicates (n = 40). For microbiome and enzymatic analyses, we sampled soil from two soil layers i.e., 0-30 cm and 30-60 cm of three plant replicates (n = 12). Following soil sampling, the roots were carefully extracted and washed over a 1-mm sieve to retrieve most of the root system. They were stored in 30% (v/v) ethanol before analysis. They were then scanned at 600 dpi (Epson Perfection V800 Photo, Epson, Japan) and analyzed with the WinRhizo® software (Regent Instruments Inc., Quebec, Canada).

All plant biomass was oven-dried at 60 $^{\circ}$ C to constant weight for three days before determining the dry weight. The plant material was then ball-milled (MM 400, Retsch, Germany) and weighed into tin capsules (HEKAtech, Wegberg, Germany) for C and 15 N content determination using an elemental analyzer coupled to an isotope-ratio mass spectrometer (EA-IRMS, Flash EA 2000, coupled to Delta V Plus; Thermo Fisher Scientific, Waltham, MA, USA).

2.4. Processing of soil samples

Soil samples were extracted with 0.01 M CaCl $_2$ (soil-to-solution ratio of 1:4 w:v), vortexed, shaken horizontally for 2 h at 200 rpm, centrifuged for 15 min at $690\times g$, and filtered through 0.45 µm PP-membrane filters (Ø 25 mm; DISSOLUTION ACCESSORIES, ProSense B·V., München, Germany). Soil solution was analyzed for DOC with a total organic carbon analyzer (TOC-V + ASI-V + TNM, Shimadzu, Japan). NH $_4^+$ was measured by continuous-flow analysis (Flowsys, Alliance Instruments GmbH, Freilassing, Germany). NO $_3^-$ was measured by ion chromatography (Metrohm 850 Professional IC Anion – MCS, Metrohm AG, Herisau, Switzerland). Enzymatic activity of β -glucosidase (BGU) and leucine aminopeptidase (LAP), two hydrolytic enzymes involved in soil C and N cycling, was measured as reported by Kaloterakis et al. (2024a), following German et al. (2011). The kinetics of BGU and LAP were measured by fluorimetric microplate assays of 4-methylumbelliferone (MUF) and 7-amino-4-methyl coumarin (AMC; Razavi et al., 2017).

2.5. Soil DNA extraction and 16S rRNA gene amplicon sequencing

Total genomic DNA from bacteria and archaea was extracted from 0.5 g of RA and RH soil samples using a bead-beating method according to the manufacturer's description (FastDNA SpinKit for Soil, MP Biomedicals, Eschwege, Germany) and established protocols (Braun-Kiewnick et al., 2024). DNA quantity and quality were checked by Nanodrop and on 0.8% agarose gels, and amplification efficiency of appropriate DNA dilutions (10-20 ng μL^{-1}) was tested by a pre-Illumina

PCR using a fragment of the V3–V4 region of the 16S rRNA gene with the same primers as for amplicon sequencing, except for the adaptors (Uni341F (5' CCTAYGGGRBGCASCAG 3') and Uni806R (5' GGACTACHVGGGTWTCTAAT 3')) (Yu et al., 2005; Caporaso et al., 2011; Sundberg et al., 2013). PCR products were checked on 1% agarose gels before sending genomic DNA to amplicon sequencing (Novogene, Cambridge, UK). Amplicon libraries with the primers Uni341F-Uni806R and Illumina adaptors (Illumina, San Diego, USA) were then generated and sequenced at Novogene using Illumina MiSeq v2 (2 x 250 bp) chemistry according to the manufacturer's instructions (Illumina, San Diego, USA). Unassembled raw amplicon data were deposited at the National Center for Biotechnology Information (NCBI) Sequence Read Archive (SRA) under PRJNA1146588.

2.6. Amplicon sequence analyses

The downstream analysis was conducted in R (v4.2.1; R Core Team, 2022). The amplicon sequencing analysis was performed in the Divisive Amplicon Denoising Algorithm (DADA2 v.1.12.1 pipeline; Callahan et al., 2016). A total of 1,668,656 high-quality reads with a maximum of two expected errors were retained from 32 samples corresponding to eight plants, two soil layers 0-30 cm and 30-60 cm and two soil compartments i.e., RH and RA. The taxonomic classification of amplicon sequence variants (ASVs) was conducted using the SILVA database v.138 (Quast et al., 2013) and the 'phyloseq' package (McMurdie and Holmes, 2013). Unassigned ASVs at the phylum level and any remaining ASVs identified as chloroplasts, mitochondria, or eukaryotes were omitted from the studies. A taxonomic level called "Annotation" was manually included in the taxonomic table, which included the latest taxonomic information for each ASV. The dataset was subjected to rarefaction analysis to ensure an equal level of sequencing depth (Schloss, 2024), with the minimum number of sequences (34,391) observed in all samples. The rarefaction curves tended to reach a plateau, indicating that the sequencing method supplied sufficient sequences to cover most of the sample diversity.

Alpha diversity indices were calculated using the 'phyloseq' and 'microbiome' packages (Lahti and Shetty, 2017). Significant changes were determined using Kruskal-Wallis tests and post-hoc Wilcoxon-Mann-Whitney tests. The analysis of beta diversity employed square root transformed ASV count data using the 'vegan' package (Oksanen et al., 2022) and was visualized through multidimensional scaling (MDS) plots. The study evaluated variations in beta diversity centroids by applying permutational multivariate analysis of variance ('adonis'). PERMANOVA tests, and ANOSIM. Differential abundance (DA) analysis was performed using DESEeq2 negative-binomial Wald test (Love et al., 2014). Taxa were considered significant if their adjusted p-value was less than 0.05 after the Benjamini-Hochberg correction. Additionally, the putative prediction of the functions of the bacterial and archaeal communities from 16S rRNA gene sequencing data was performed using the software Tax4Fun2 v1.1.5 (Wemheuer et al., Log-transformed data from the differentially abundant taxa in each group of samples were used to obtain predicted relative values for different KEGG orthologues. KEGG functional pathways and nitrogen metabolism genes were selected based on five keywords, "nitrogen", "ammonium", "ammonia", "nitrate", and "nitrite".

2.7. Quantification of total bacteria (16S rRNA), bacterial 16S rRNA amoA (AOB) nirS, nosZ, and nifH genes and archaeal 16S rRNA and amoA genes (AOA) by qPCR

Quantitative PCR (qPCR) was used to measure the absolute abundance of bacterial 16S rRNA gene copies and N cycle-related genes, including the ammonia monooxygenase (AMO) alpha subunit (amoA), NO_2^- reductase (nirS), nitrous oxide reductase (nosZ), and N_2 -fixing nitrogenase (nifH) genes in both RA and RH samples. To quantify absolute bacterial abundance, the BACT1369F, PROK1492R, and

TM1389F primers, labeled with 5'-FAM and 3'-TAMRA, were used in a specific TaqMan assay, following the protocol described by (Suzuki et al., 2000). To determine the absolute abundance of the bacterial amoA gene (AOB) the primers amoA-1F and amoA-2R developed by (Rotthauwe et al., 1997) were employed as described in Meyer et al. (2013). For quantifying the nirS gene the primers cd3aF and R3cd (Throbäck et al., 2004), and for the nifH gene, the forward primer FPGH19 (Simonet et al., 1991) was used along with the reverse primer PolR (Poly et al., 2001). Finally, for the nosZ gene quantification, the nosZ-2F and nosZ-2R primers were used (Henry et al., 2006). All reactions were conducted in a total volume of 20 μL containing 10 $\mu :$ of 2 xLuna Universal qPCR Master Mix (New England Biolabs, Ipswich, USA), $0.1 \text{ mg mL}^{-1} \text{ BSA}$, 200 nM (amoA) or 400 nM (nirS, nifH, nosZ) of each primer and 5 µL of template DNA (1:5 diluted) per reaction. PCR cycling conditions were 1 min at 95 °C, followed by 40 cycles of 15 s at 95 °C and 30 s at 60 °C. The specificity of the amplification products employing SYBR green chemistry (New England Biolabs, Ipswich, USA) was confirmed through melting curve analyses after completion of amplification cycles (60°C–95 °C, Δ 0.5 °C every 5 s).

The quantification of all target gene copies in the samples was determined by comparing them to adequate standard curves of cloned and purified target gene copies, and all measurements were based on 1 g of soil (gene copies per g of soil). Standard curves were generated by serial dilutions of target genes (ranging from 10^{-2} to 10^{-7}). Reference DNAs for bacterial nirS, nifH, nosZ, and amoA genes were used based on purified gene fragments inserted into either the pEASY-T1 (nirS, nifH, nosZ) or pCR2.1 (amoA) cloning vectors and transformed into E. coli. All measurements were run in duplicates (= technical replications) on a CFX96 Real-Time System (Bio-Rad, Laboratories GmbH, München, Germany). Precautions were taken to ensure that the data from each duplicate fell within 0.5 threshold cycle (Ct), and clear outliers (> 2 standard deviations) were removed before calculating the average Ct of each treatment, with each treatment having three biological replications, resulting in six data points per measurement. Melting curves and non-template controls were used to assess run reliability. There was no detectable amplification arising from non-template controls in any of the assays. The amplification efficiencies of all qPCR assays ranged from 91% to 98%, calculated from the equation:

$$\mathit{Eff} = 10 \times \left(\frac{-1}{\mathit{slope}}\right) - 1$$

Archaea-specific qPCRs were conducted to quantify total archaea and amoA (AOA) gene copies of archaea, archaea-specific qPCRs were conducted. To quantify the absolute abundance of archaea, the ARC787F_YU, ARC1059R_YU, and ARC915F_YU probe (with 5'-FAM and 3'-TAMRA labels) were used in a TaqMan assay, following the protocol described by (Yu et al., 2005). For quantification of the archaeal ammonia monooxygenase alpha subunit (amoA) the forward primer amo19F (Leininger et al., 2006) and reverse primer CrenamoA616r48x (Schauss et al., 2009) were used according to the protocol described by Meyer et al. (2013). PCR reactions were conducted in a total volume of 20 µL, containing 10 µL of 2 x Luna Universal qPCR Master Mix (New England Biolabs, Ipswich, USA), 0.1 mg mL⁻¹ BSA, 600 nM of each primer and 5 μl of template DNA (1:5 diluted, ca. 10-20ng μL⁻¹) per reaction. PCR cycling conditions were 10 min at 94 °C, followed by 40 cycles of 45 s at 94 $^{\circ}$ C, 45 s at 60 $^{\circ}$ C, and 45 s at 72 $^{\circ}$ C. The specificity of amplification products employing SYBR green chemistry was confirmed through melting curve analyses after completion of amplification cycles (72–95 $^{\circ}$ C, Δ 0.5 $^{\circ}$ C every 5 s). The quantification of target gene copies was conducted as described above, and reference DNA for total archaea was based on 10-fold serial dilutions of purified PCR product 16S rRNA gene from Methanobacterium oryzae (ca 1300 bp, cloned into pGEM-T transformed in E. coli). Reference DNA for the archaeal amoA gene (AOA) was based on 10-fold serial dilutions of purified archaeal amoA gene fosmid clone 54d9 (656 bp) from

Crenarchaeota cloned into pCR2.1 and transformed into *E. coli*. Calculations of total archaea and AOA gene copy numbers were performed as described above.

2.8. Data analysis

After assessing normality and homogeneity of variances using the Shapiro-Wilkinson and Levene test, respectively, we conducted ANOVA with the Bonferroni correction at $p \leq 0.05$, using the rotational position of WW (two levels) and soil depth (three levels) as fixed factors. When the assumptions of normality were not met, we transformed the data using the Yeo-Johnson transformation (Yeo and Johnson, 2000). The transformation used for a certain variable is mentioned in the respective table. Data analysis was performed with IBM SPSS Statistics for Windows, version 23 (IBM Corp., Armonk, NY, USA). The packages 'ggplot2' (Wickham, 2016) and 'ggstatsplot (Patil, 2021) in R were used to create the graphs and correlograms of Spearman rank correlation matrices.

3. Results

3.1. Soil mineral N and enzymatic activity at tillering and grain ripening growth stage

At T1, the rotational position of WW strongly influenced soil NO₃ (p = 0.002), soil NH₄⁺ (p = 0.001), BGU (p < 0.001) and LAP activity (p = 0.001) 0.007), while soil depth affected only soil NO $_3^-$ (p < 0.001; Table S1). More specifically, we measured 55.9% higher NH₄ in the soil of W2 compared to W1, which was mainly evident in the 0-30 cm and 30-60 cm layers of the soil (Fig. 1a). In the soil of W1, NO₃ was on average 87.5% higher than in W2, mainly due to large differences in the deep subsoil of 60-100 cm (Fig. 1b). With respect to enzymatic activity, BGU V_{max} of W2 was 351.4% higher than in W1, with significant differences in both 0-30 cm and 30-60 cm layers (Fig. 1c). The opposite trend was recorded for LAP V_{max} with an 18.3% reduction in W2 compared to W1 (Fig. 1d). At T2, the rotational position of WW significantly influenced soil NO_3^- (p < 0.001) and soil NH_4^+ (p = 0.001), while BGU and LAP activity remained unaffected (Table S1). Soil depth had the same main effect on soil NO_3^- (p = 0.015) and soil NH_4^+ (p < 0.001), with no effect on BGU and LAP activity. We recorded a 24.0% higher NH₄⁺ content in the soil of W1 compared to W2 (Fig. 1e) while the opposite was detected for NO_3^- , with a 51.2% reduction in W1 compared to W2 that was evident throughout the soil profile (Fig. 1f). No differences were observed for the enzymatic activity of BGU and LAP between the rotational positions (Fig. 1g and h).

3.2. N-related genes at the tillering and grain ripening growth stage

At T1, there was no significant influence of the rotational position of WW on the absolute abundance of 16S gene copy numbers for both bacteria (Fig. 2a-e; Table S2) and archaea (Figs. S4a and d; Table S3) at both WW developmental stages. In contrast, the rotational position of WW (p = 0.017) and soil depth (p < 0.001) had a significant main effect on the amoA gene copy number of AOB (Table S2), with a much higher amoA abundance in the topsoil of W2 compared to W1 (Fig. 2b). We also noted a significant increase of bacterial nifH gene copy numbers only in the topsoil of W2 compared to W1 (Fig. 2c). In addition, both the rotational position of WW (p < 0.001) and soil depth (p < 0.001) significantly influenced bacterial nirS gene copy numbers, with higher bacterial nirS abundance in both the top and subsoil of W2 compared to W1 (Fig. 2d). At T2, the main effects of rotational position of WW and soil depth were insignificant (Table S2). However, we did find higher amoA copy numbers of AOB and a higher bacterial nirS gene abundance in the topsoil of W2 compared to W1 (Fig. 2f-h). At the same time, no differences were evident for bacterial nifH gene abundance at this late growth stage (Fig. 2g). Finally, no differences were found in amoA gene copy number of AOA (Figs. S4b and e) and bacterial nosZ gene

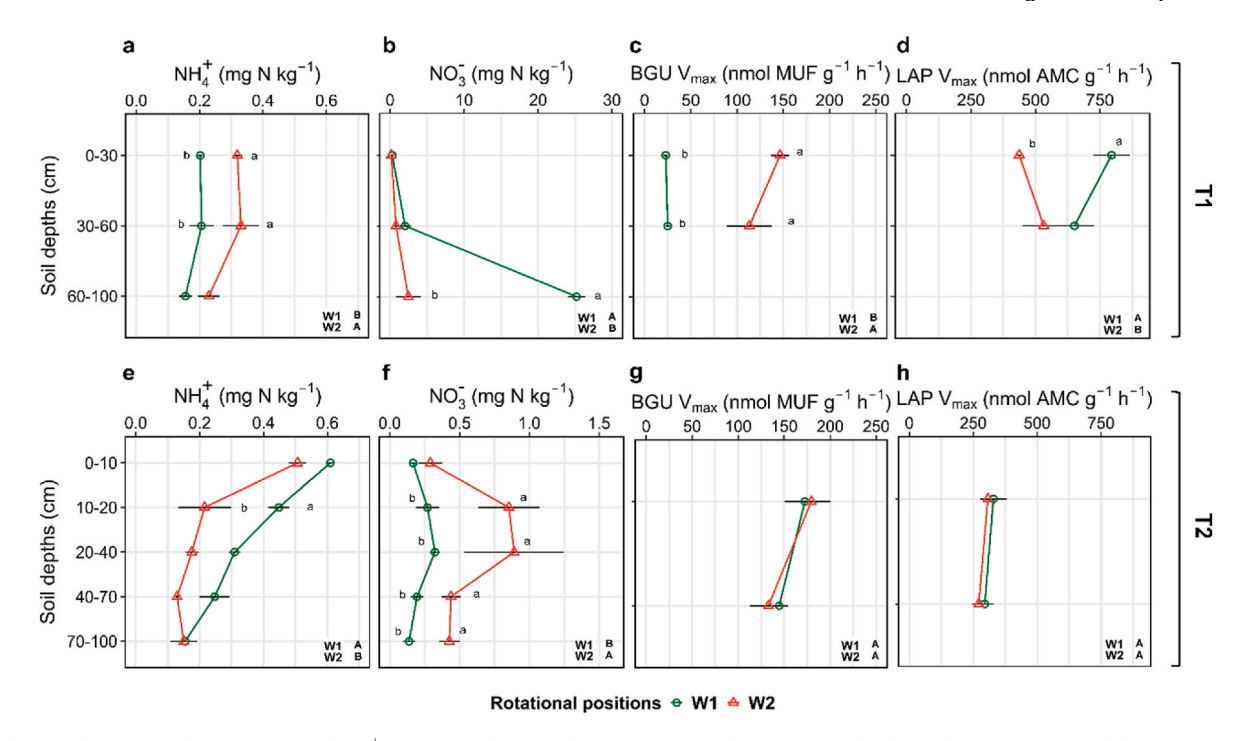


Fig. 1. Effect of the rotational positions on soil NH_4^+ -N (a, e), soil NO_3^- -N (b, f), maximum velocity (V_{max}) of β -glucosidase (BGU; c, g) and leucine aminopeptidase (LAP; d, h) of the following winter wheat at tillering (BBCH 29, 28 DAS) and grain ripening (BBCH 90, 180 DAS). W1 = first wheat, W2 = second wheat after oilseed rape. Different uppercase letters in each subplot indicate significant differences between the rotational positions. Within each soil depth, different lowercase letters denote significant differences between rotational positions at $p \le 0.05$. Four plant replicates were analyzed for mineral N (n = 48 for T1 and n = 40 for T2) and three plant replicates were analyzed for BGU and LAP (n = 24 for T1 and n = 12 for T2).

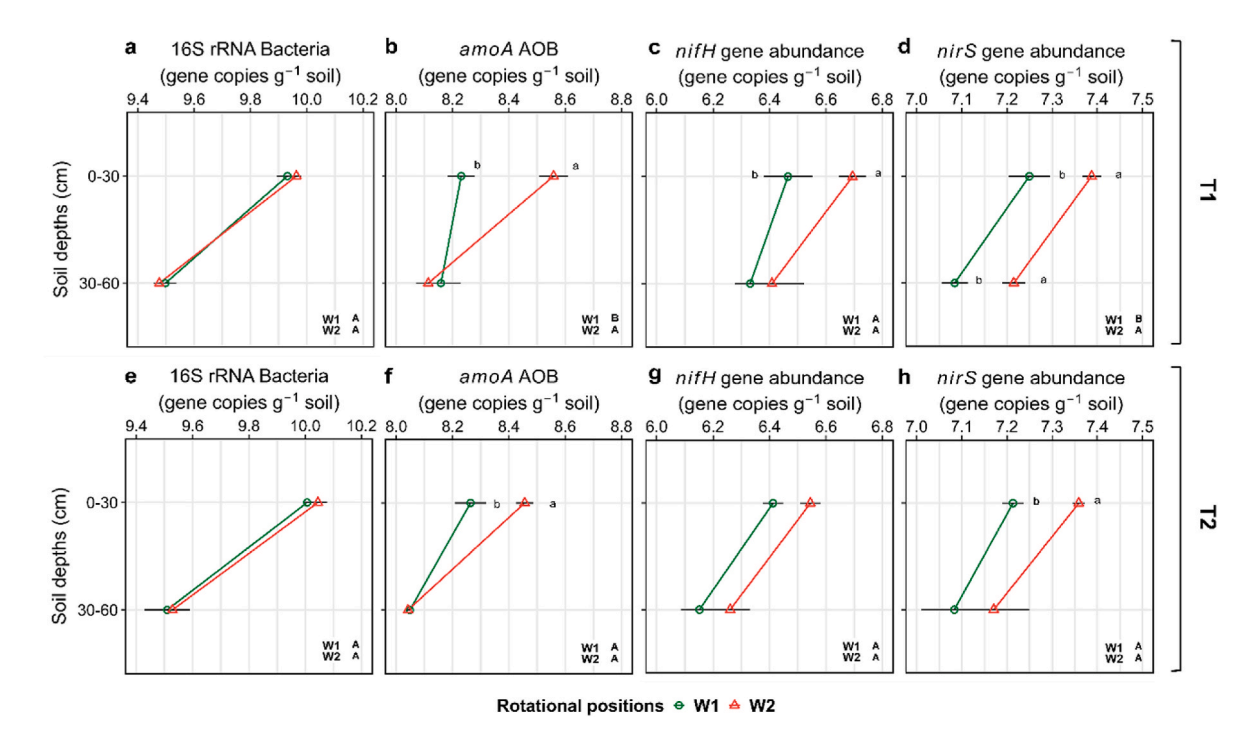


Fig. 2. Effect of the rotational positions on the 16S rRNA gene copy number of Bacteria (a, e), ammonia-oxidizing bacteria *amoA* gene abundance (AOB; b, f), bacterial *nifH* gene abundance (c, g) and bacterial *nirS* gene abundance (d, h) of the following winter wheat at tillering (BBCH 29, 28 DAS) and grain ripening (BBCH 90, 180 DAS). W1 = first wheat and W2 = second wheat after oilseed rape. Different uppercase letters in each subplot indicate significant differences between the rotational positions. Within each soil depth, different lowercase letters denote significant differences between rotational positions at $p \le 0.05$. Three plant replicates were analyzed for the response variables (n = 24 for T1 and n = 12 for T2).

abundance (Figs. S4c and f) between the rotational positions and the sampling time points (Table S3).

3.3. Characterization of the bacterial and archaeal communities

We used 16S rRNA gene amplicon sequencing to characterize the bacterial and archaeal communities obtained from different samples. No significant differences in alpha diversity (microbial diversity within samples) were observed between the specific bacterial and archaeal communities of W1 and W2 at T1 or T2 across all microhabitats (Fig. 3a). Regarding beta diversity (comparison among communities), depth and rotation were the primary factors influencing the soil bacterial and archaeal diversity and composition at T1 (Bray-Curtis distances, Depth, $R^2 = 0.10$; Rotation, $R^2 = 0.07$; p < 0.001) (Fig. 3b). Since the microhabitat (RH and RA) was the variable that affected the bacterial and archaeal communities the least (contributing to 5.2% of the variation; p < 0.040), samples were combined. At T2, without sampling across different microhabitats, rotation and depth continued to shape the soil microbial diversity and composition across different rotational positions (Fig. 3c, Depth, $R^2 = 0.16$; Rotation, $R^2 = 0.15$; p < 0.001). The ten most abundant taxa, including Bacillus, Gaiella, and Sphingomonas, were the same at T1 and T2, except for a taxon belonging to the family Methyloligellaceae (among the top 10 in T1) and a taxon from the

Subgroup 7 (Acidobacteriota; Holophagae; among the top ten at T2). A taxon belonging to the archaeal family Nitrososphaeraceae presented an overall relative abundance of 1.1% of the total sequences.

When comparing the effect of WW rotational positions on the bacterial and archaeal communities at different plant developmental stages and depths, we observed that significantly more taxa were differentially abundant at T1 than at T2 (Fig. 4). At T1 and in the 0-30 cm soil layer, eleven out of twelve differentially abundant taxa were more prevalent in W1, including Corynebacterium, Moraxella, Neisseria, Noviherbaspirillum, and a taxon belonging to the family Xanthobacteraceae. Tumebacillus was the only taxon significantly more abundant in W2 (Fig. 4a). At T1 and in the 30-60 cm soil layer, twelve taxa were significantly more abundant in W1 than W2, including Phenylobacterium and a taxon belonging to the family Xanthobacteraceae. Conversely, four taxa, including Dyella and Rhodobium, were more abundant in W2. Notably, Phenylobacterium and a taxon from the family Xanthobacteraceae were consistently more abundant in W1 at both depths. At T2, Shinella was significantly more abundant in W1 than in W2 in the 0-30 cm soil layer. while the cluster ANPR, Acinetobacter, and a taxon from the family Devosiaceae were more abundant in W2 than W1 (Fig. 4b). Interestingly, Caulobacter, Gemmatimonas, Streptomyces, and Verrucosispora were more prevalent in W1 compared to W2. In contrast, Devosia and a taxon from the same family, Devosiaceae, were among the taxa significantly

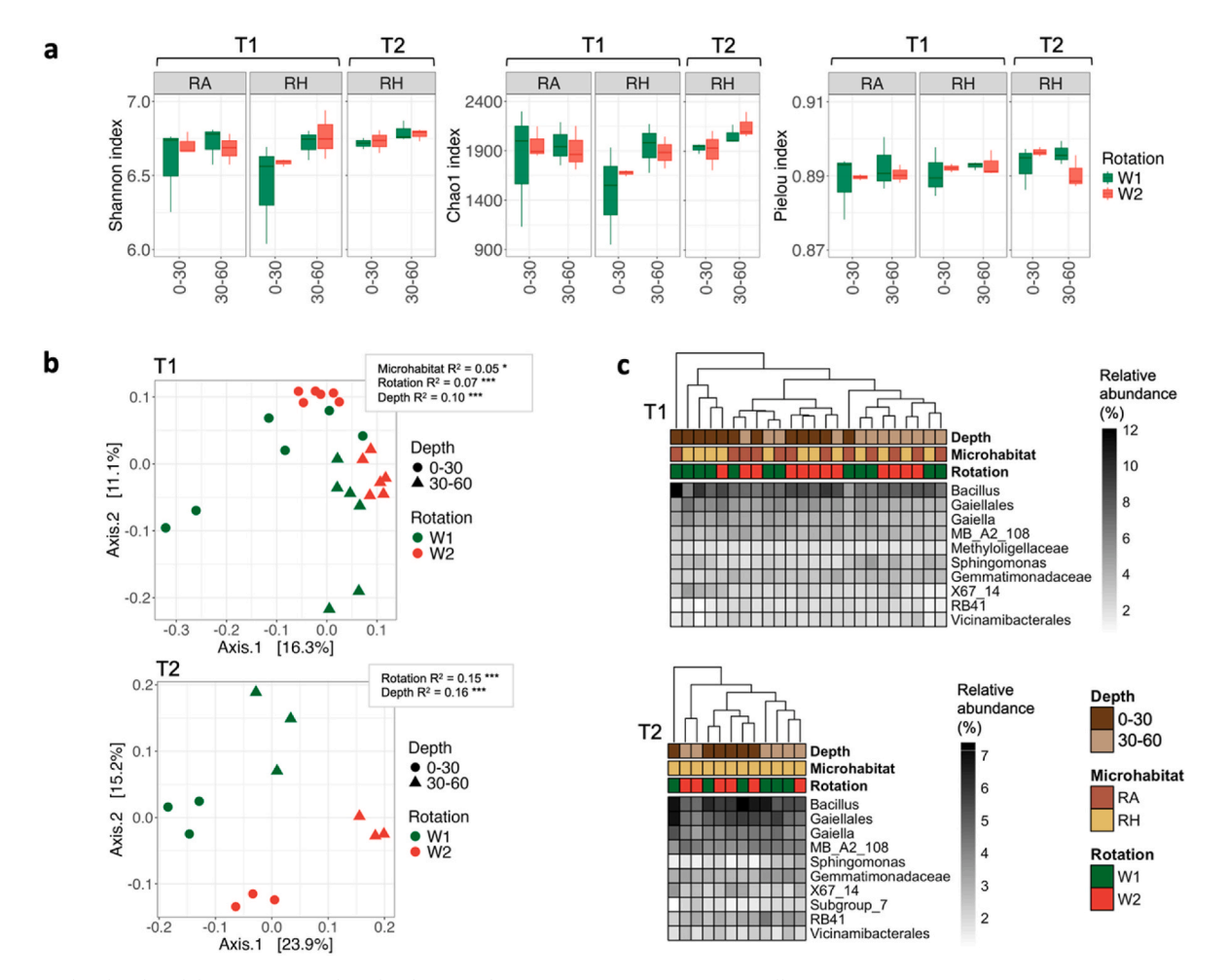


Fig. 3. Bacterial and archaeal diversity at two plant developmental stages (T1 = BBCH 29, 28 DAS, tillering; T2 = BBCH 90, 180 DAS, grain ripening), separated by soil depth (0–30 cm; 30–60 cm), microhabitat (RA = root-affected soil; RH = rhizosphere), and rotational position (W1 = first wheat after oilseed rape; W2 = second wheat after oilseed rape), based on 16S rRNA gene amplicon sequencing data. (a) Alpha diversity metrics, including Shannon's diversity, Chao1's richness, and Pielou's evenness (analyzed using the Mann–Whitney U test with p-values adjusted by the Bonferroni method). Vertical bars represent standard errors. (b) Beta diversity was measured using Bray-Curtis dissimilarity and visualized through multidimensional scaling (MDS), with statistical analysis performed using PERMA-NOVA. (c) Relative abundance of the ten most prevalent taxa in T1 and T2. Significance levels: *p < 0.05; ***p < 0.001. Three plant replicates were analyzed for the response variables (n = 24 for T1 and n = 12 for T2).

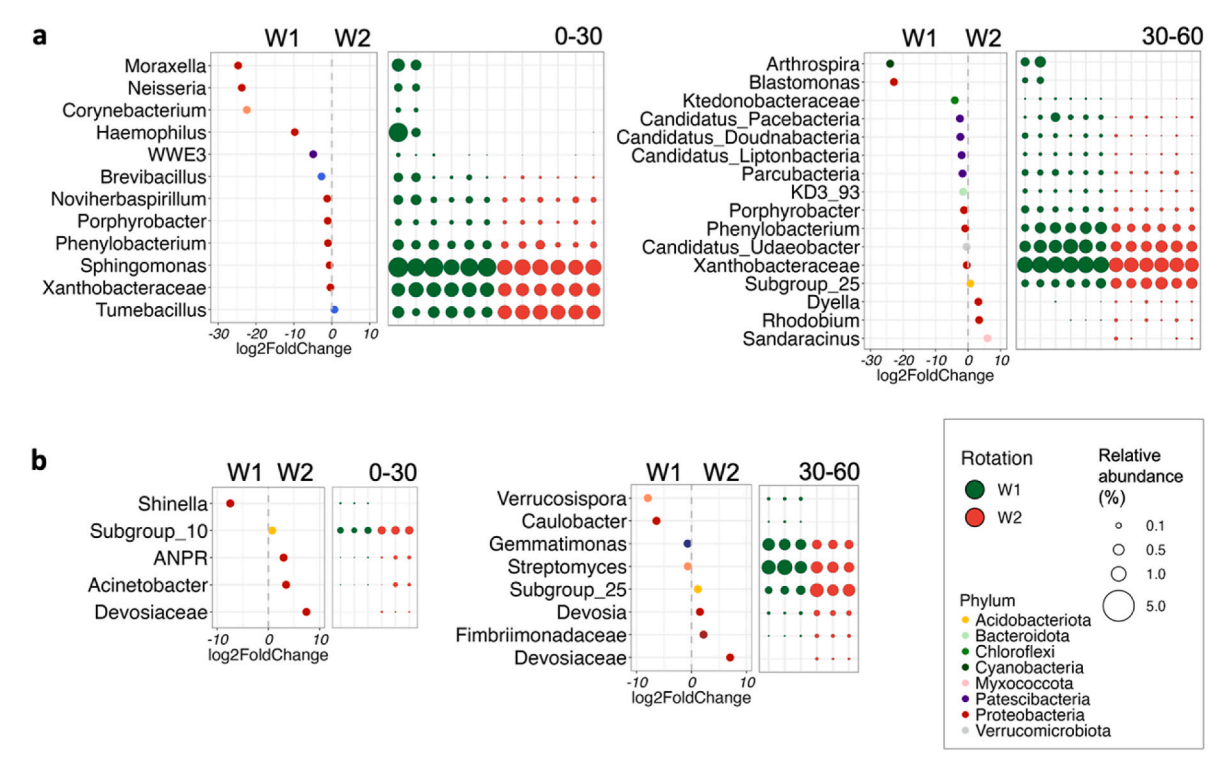


Fig. 4. Differentially abundant (DA) taxa between crop rotational positions (W1 = first wheat after oilseed rape as a pre-crop; W2 = second wheat after oilseed rape) at two plant developmental stages: (a) T1 (BBCH 29, 28 DAS, tillering) and (b) T2 (BBCH 90, 180 DAS, grain ripening), separated by soil depth (0–30 cm; 30–60 cm). The lowest confident taxonomic classifications are shown, with each corresponding phylum represented by a unique color. Negative log2FoldChange values indicate a significantly higher abundance in W1, while positive log2FoldChange values indicate a higher abundance in W2. The relative abundance of each significantly different taxon is depicted by round shapes, varying in size from 0.1% to 3% of the total sequences. p values < 0.05 were adjusted using the Benjamini-Hochberg correction. Three plant replicates were analyzed for the response variables (n = 24 for T1 and n = 12 for T2). (For interpretation of the references to color in this figure legend, the reader is referred to the Web version of this article.)

more abundant in W2 than W1.

Using Tax4Fun2, we searched for the relative abundance of N-related genes that matched genes related to nitrate, nitrite (NO_2^-) or ammonia/ammonium metabolism in the differentially abundant taxa in each group of samples. No statistical significance was found between depths or rotations (p>0.05), except for the decrease in N-related genes in 30–60 cm compared with 0–30 cm in W2 at T1 (p=0.002) (Fig. S1a). N metabolism regulators, regulatory proteins and components of the NtrC gene family were found in higher abundance at T1, either W1 or W2 samples (p<0.01) (Fig. S1b). Nitrate/nitrite response regulators belonging to NarL are significantly higher in T2, 30–60 cm (p=0.004), so as the assimilatory nitrate reductase.

Correlation analyses at T1 and in the 0–30 cm soil layer revealed a significant positive correlation between NO_3^- and *Moraxella*, *Neisseria*, *Corynebacterium* and *Haemophilus* in W1, but not in W2 (Fig. S2). In this soil layer, BGU V_{max} was also positively correlated with LAP V_{max} in W1, but not in W2. Gene abundance of bacterial nifH and nirS in the topsoil of W2 was positively correlated with *Porphyrobacter* and *Noviherbaspir-illum*, respectively, while this was not the case for W1. In the 30–60 cm soil layer, we found a positive correlation between NO_3^- and *Rhodobium* in W1, while in W2 they were negatively correlated (Fig. S3). Bacterial nifH gene abundance positively correlated with *Arthrospira* and *Blastomonas* in W1 and with *Candidatus* Doudnabacteria in W2.

3.4. Effect of rotational position on WW biomass accumulation and root growth

The rotational position of WW had a strong effect on plant biomass accumulation. W1 produced 51.5% more biomass than W2 (p < 0.001; Table S4), mainly due to differences in grain, husk and root dry weight (Fig. 5a). Overall, C:N ratio remained unaffected by the rotational

position of WW, but W2 had a higher stem C:N ratio compared to W1 (Fig. 5b). Regarding root growth traits we noted a significantly higher root dry weight (p < 0.001; Table S5; Fig. 5c) and root mass density (p < 0.001; Fig. 5d) in W1 compared to W2, which was evident throughout the soil profile. Fig. 5c and d have been adapted from Kaloterakis et al. (2024a).

4. Discussion

4.1. Distinct soil legacies of the preceding crops on WW growth

The rotational position of WW modulated changes in soil nutrient content, microbial community structure and enzymatic activity, which ultimately translated into yield discrepancies. Given that at the early growth stage of T1 the root system was mainly located in the upper 50 cm of the rhizotrons, the higher NO₃ content in the 60–100 cm of W1 can be directly linked to the initial soil NO₃ content at the start of the experiment and the microbial activity (Kaloterakis et al., 2024a). The N-rich residues of oilseed rape (with a lower C:N compared to WW) were mineralized faster, creating an N-rich environment for the following WW. This is also supported by the enhanced LAP activity in W1 compared to W2. LAP activity degrades proteins into amino acids that can be further degraded into ammonia. This higher activity in W1 is likely due to the protein-rich organic material of oilseed rape residues that were decomposing in the soil during WW growth, thus contributing to the higher NO₃ levels in the soil of W1. On the contrary, the increased BGU activity in W2 compared to W1 can be expected due to the higher C: N ratio of WW residue with a higher cellulose content than that of oilseed rape. At T1, BGU Km was significantly affected by WW's rotational position and it was significantly higher in W2 compared to W1 meaning that the soil microbes in W2 had a much lower enzymatic

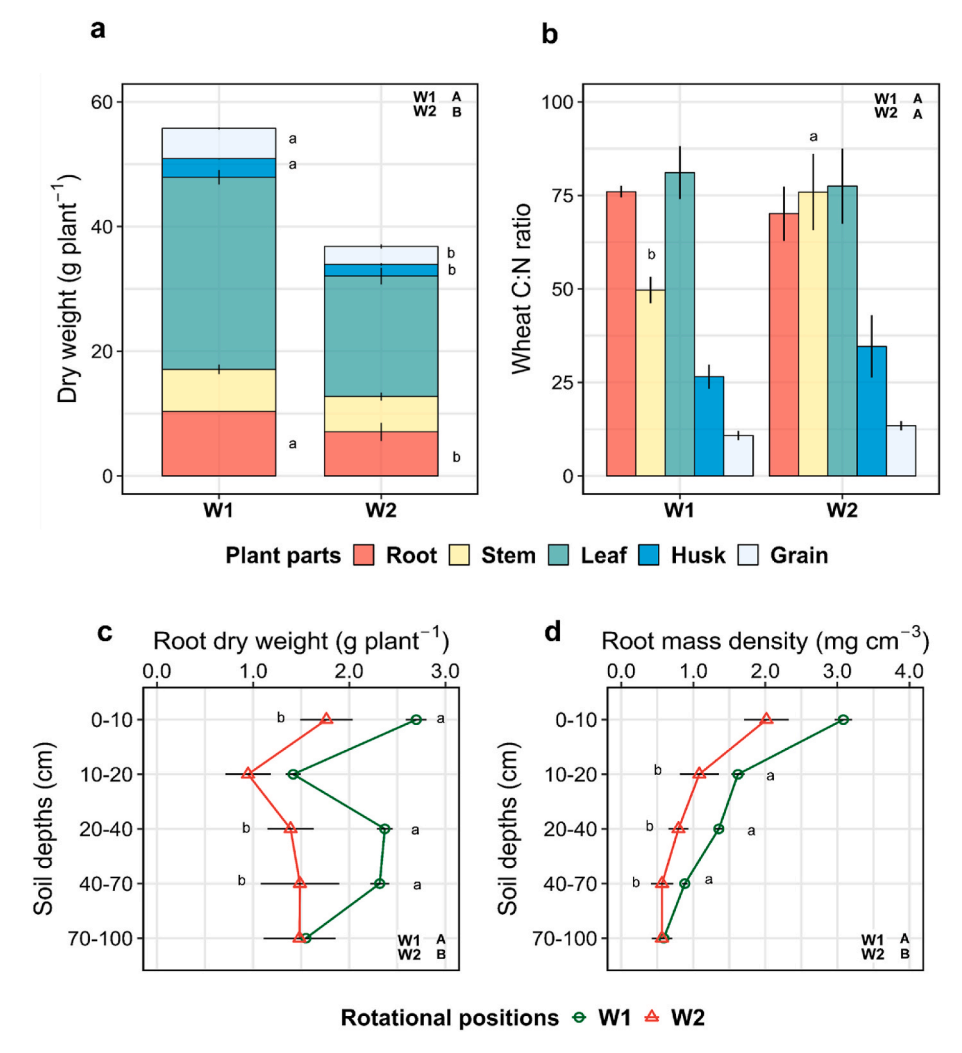


Fig. 5. Effect of the rotational positions on root, stem, leaf, husk and grain dry weight (a), C:N ratio (b), root dry weight (c), and root mass density (d) of the following winter wheat at grain ripening (BBCH 90, 180 DAS). W1 = first wheat, W2 = second wheat after oilseed rape. Different uppercase letters in each subplot indicate significant differences between the rotational positions. Within each plant part (panels a, b) and soil depth (panels c, d) different lowercase letters denote significant differences between rotational positions at $p \le 0.05$ level according to ANOVA with Bonferroni correction for multiple comparisons. Fig. 5c and d adapted from Kaloterakis et al. (2024b). Four plant replicates were analyzed for the response variables (n = 40 for the response variables).

affinity for BGU than those in W1 (Table S6). This means that BGU was released by different microbial groups despite the lack of a significant shift in the bacterial and archaeal community composition. The absence of significant differences for LAP Km indicates that the bacterial and archaeal communities of W1 and W2 produced more enzymes to degrade the protein-rich organic material in the soil. At T2, both BGU and LAP were released by different microbial groups in W1 and W2, as shown by the significant effect of the WW's rotational position of BGU and LAP $\rm K_m$ (Table S6).

The soil microbes in the soil of W2 are faced with an early N immobilization in its rhizosphere, which has been previously observed during the early growth of successively grown WW (Kaloterakis et al., 2024b). In the same study, the authors also recorded a much lower root growth in the successive WW rotation, which negatively correlated with soil NH $_4^+$ as opposed to WW after oilseed rape. Although we did not measure root growth at T1, we nevertheless detected less NH $_4^+$ in the 0–30 cm and 30–60 cm layers of the soil profile in W1 compared to W2, which might reveal the same mechanism given that we used the same soil from the same experimental plots as Kaloterakis et al. (2024a). This points towards the early disadvantage of the successive WW rotation in accessing available mineral N, and conversely the advantage of W1 with much higher NO $_3^-$ in the deep subsoil of 60–100 cm that is available for plant uptake at later growth stages when the root system is more

advanced and the subsoil nutrient and water reserves become increasingly important. Under these temporary N-limiting conditions of W2 soil, increasing BGU activity could be a way for the soil microbes to accelerate the breakdown of the cellulose-rich WW residues.

Regarding the soil legacy of the preceding crop on the bacterial and archaeal alpha diversity, we expected that the rotational position of WW would exert control over the shape of the bacterial and archaeal community structure. We did not find differences in the diversity and richness metrics of the microbial community between the rotational positions of WW, which is consistent with other studies assessing the effect of the rotational position of WW on bacterial and archaeal diversity (Braun-Kiewnick et al., 2024; Giongo et al., 2024; Kaloterakis et al., 2024b). In contrast, both the rotational position of WW and soil depth had a strong influence on beta diversity in accordance with previous studies (Town et al., 2023; Giongo et al., 2024; Kaloterakis et al., 2024b). The effects on alpha and beta diversity were similar throughout the growth cycle of WW, measured at the tillering and grain ripening stages. It should be noted that we did not measure the fungal diversity and composition, which is considered an additional or complementary driver of the observed yield reduction in the successive crop rotations (Gao et al., 2019; Wang et al., 2019; Sun et al., 2023; Town et al., 2023; Yu et al., 2024).

The differential abundance analysis revealed important shifts in the

microbial taxonomic composition, which influenced soil enzymatic activity, N cycling processes and root growth of the following WW. Although our methodology did not allow us to attribute functions to specific microbial groups, we were able to discuss potential functions of previous studies in relation to our study. Town et al. (2023) found a consistent bacterial community composition between monocropped WW and WW after oilseed rape or pea, which contrasts with our findings, possibly due to differences in soil type, which strongly affects microbial assemblages. In our experiment, Moraxella was significantly more abundant in the 0-30 cm soil layer in W1 than in W2, at tillering. This is consistent with its role in denitrification (Zheng et al., 2023), which is in line with the higher soil NO₃ content in W1 at this growth stage. Neisseria abundance has been shown to increase in a WW-maize rotation compared to monocropped WW (Navarro-Noya et al., 2013). Neisseria is known to enhance cellulose hydrolysis (Sakai et al., 1996), which could have contributed to the higher LAP activity in W1 at T1. The same is true for *Noviherbaspirillum* which includes bacterial species that are involved in cellulose degradation (Maheshwari et al., 2023). Bacilio-Jiménez et al. (2001) linked a Corynebacterium species with endophytic growth and growth enhancement in rice, which we found to be significantly more abundant in the topsoil of W1 than W2 at T1 and could have stimulated plant growth at this stage. Certain Brevibacillus species have been found to promote organic sulfur and N mineralization, increasing soil NH₄⁺ content, which boosts plant growth (Santana et al., 2013, 2021). This is consistent with the higher soil NH₄ content in W1 at T2, suggesting that the Brevibacillus may be an important genus in the degradation of the protein-rich residues of oilseed rape, thereby increasing mineral N availability for W1 uptake. Adesina et al. (2007) highlighted the antagonistic effect of Brevibacillus against Rhizoctonia solani and Fusarium oxysporum, which are important WW pathogens. Kaloterakis et al. (2024b) suggested that a more beneficial microbial community in W1 might be due to the selection of antagonists that confer protection against soil pathogens. Members of the Xanthobacteraceae family are known to be positively correlated with protease activity and soil DOC (Imparato et al., 2016), thus affecting N cycling and mineral N availability, which was evident in our study by the higher LAP activity at T1 and the higher soil NH₄ at T2 in W1.

At the grain ripening stage, we observed a much lower number of differentially abundant taxa at both soil depths compared to the tillering stage, with limited information in the literature about the potential functions of the different taxa. *Devosia* species are plant-beneficial bacteria (Jeewani et al., 2021; Cerecetto et al., 2024) with antifungal properties (Chen et al., 2022), capable of N fixation (Wolińska et al., 2017), which is in line with the higher *nifH* gene abundance in W2 at T1. Their higher abundance in the subsoil of W2 compared to W1 could be the reaction of W2 plants to enrich their rhizobiome with beneficial microbes due to the potential microbial dysbiosis in the soil that is frequently reported for monocropping systems (Zhou et al., 2023; Giongo et al., 2024). *Gemmatimonas*, a genus associated with organic matter decomposition and high gene copy numbers found in nutrient-rich soils (Banerjee et al., 2016), was more abundant in the subsoil of W1 compared to W2.

4.2. The effect of the rotational position of WW on N cycling

We hypothesized that due to changes in soil microbial community structure between the two rotational positions of WW would be accompanied by varying N-related gene abundances. Therefore, we investigated specific functional genes involved in soil N cycling as indicators of ecosystem functionality, involved in key N cycling processes in agricultural soils exposed to single or successional WW cropping. Ammonia oxidation is the rate-limiting step of nitrification, converting ammonia to NO_2^- , and is catalyzed by AMO, which is encoded by the *amoA* gene (Alves et al., 2018). Elevated *amoA* gene copy numbers have been shown to be positively correlated with the relative abundance of NO_2^- oxidizers from the phylum Nitrospirota (Daims et al., 2015). No

differences were observed between W1 and W2 for amoA of AOA, which suggests that AOB were the main ammonia oxidizers in both soils (Sterngren et al., 2015). This is in accordance with previous studies reporting a less important role of AOA in soils with high mineral fertilization (Levičnik-Höfferle et al., 2012; Chen et al., 2023). The higher initial NH $_4^+$ in W2 at T1 could have stimulated the amoA of AOB, due to the increase in available substrate for oxidation. This stimulated nitrification in response to the increased NH $_4^+$ availability from the decomposing residues of the preceding WW. Over time, this trend weakened, as shown by the insignificant overall main effect of the rotational position on amoA of AOB at T2 and the higher NH $_4^+$ in W1 than W2.

Bacterial nirK and nirS genes encode NO-producing NO₂ reductase. NO is then reduced to N₂O during denitrification, further reduced to N₂ by nitrous oxide reductase encoded by nosZ (Zumft, 1997). Liu et al. (2023) described crop rotation as an important moderator of N-related genes. Both nirK and nirS are considered important predictors of N losses via N₂O emissions (Yang et al., 2022; Giongo et al., 2024) assessed the relative abundance of bacterial N-cycling genes in the root-affected, rhizosphere and rhizoplane soil of two rotational positions of WW, i. e., first WW after oilseed rape and a 15-year WW monocropping in silty loam Luvisol. Although soil depth was an important driver of microbial community composition, they did not find differences between the rotational positions of WW. In our study, although there was no effect of the rotational position of WW on bacterial nosZ gene copy numbers, we found a significant increase in nirS gene copy numbers in W2 in both topsoil and subsoil at tillering. nirS genes are linked to denitrification, the major N loss pathway that reduces NO₃ to N₂ or N₂O (Wei et al., 2015). The higher bacterial nirS gene abundance indicates a higher conversion of NO₂ to NO in the second step of denitrification (Wei et al., 2015) and therefore a more active denitrification in W2 compared to W1. Even though we found more NO₃ in the soil of W1 at T1, the increase of bacterial nirS gene copy numbers in W2 suggests that NO3 is rapidly used and transformed by denitrifiers and thus lost for uptake by the WW roots. Perhaps, the secretion of certain compounds derived from oilseed rape residues suppresses the denitrifiers, which in turn leads to a higher NO₃ content in the soil of W1 than W2.

A higher rate of N-fixing bacteria (increase of bacterial nifH gene copy numbers that encode for the nitrogenase enzyme) was noticed only at tillering and in the topsoil of W2 compared to W1, possibly hinting at a higher conversion of N_2 to NH_4^+ in the rhizosphere of continuous WW. These N-fixing bacteria seemed to be relatively more abundant under the N-limiting conditions of W2 (Chen et al., 2024), possibly contributing to the increase of soil NH₄ from T1 to T2, while the respective increase in soil NH₄⁺ from T1 to T2 in W1 was mainly due to enhanced root exudation, growth and turnover (Kaloterakis et al., 2024a). The microbial community is obviously adapting to the initial nutrient limitation (at least during the early growth) by shifting to more N-fixing bacteria. Plants actively participate in this interaction through root exudation to recruit N-fixing microbes under N-deficient conditions (Wassermann et al., 2023), as reflected in the exudation of flavonoids by maize under N-limiting conditions (Yu et al., 2021). The lower and higher activity of LAP and BGU, respectively, in W2, might be indicative of the response of the bacterial community to increasing soil N content by stimulating the breakdown of cellulose-rich residues of the preceding WW and increasing the abundance of N-fixing nifH genes. Under increased soil mineral N content, the relative abundance of nifH genes is known to decrease (Hao et al., 2022), similar to what we observed in the soil of W1 at T1. According to the ecological theory, at relatively higher mineral N conditions, diazotrophs will preferentially use mineral N, since it is a more energetically efficient strategy than fixing atmospheric N₂ (Contosta et al., 2011).

4.3. Contrasting drivers of soil N cycling among the rotational positions of WW contribute to yield discrepancies

In $a^{13}CO_2$ pulse labeling experiment (Kaloterakis et al., 2024a), showed that successive WW rotations invest a lower amount of photosynthates above and belowground compared to WW after oilseed rape, which contributes to reduced plant growth. They also reported a long-lasting effect of increased belowground $^{13}CO_2$ fluxes from flowering until grain ripening for WW grown following oilseed rape. Extending the outcome of this study, we show here that the positive PSF of WW grown after oilseed rape is also strongly related to its ability to utilize the residual soil mineral N pool. We argue that this is mainly due to distinct changes in the N cycling in the soil of W1 compared to W2.

At the grain ripening stage, the higher soil NH_{+}^{+} content in W1 and the lower *amoA* abundance from AOB indicate that, relative to NH_{+}^{+} , more soil NO_{3}^{-} was taken up by W1 plants compared to W2 and thus significantly less soil NO_{3}^{-} was found in W1 soil. The higher nitrification activity in W2 converted more of the available NH_{+}^{+} to NO_{3}^{-} , which was not utilized by the plants due to the reduced root growth throughout the soil profile. The higher LAP activity of W1 at tillering could have stimulated organic N mineralization, resulting in higher NH_{+}^{+} content at the end of the experiment, which was complemented by its larger root system, with a higher amount of root debris and rhizodeposition fueling the turnover of organic matter (Yang et al., 2023).

5. Conclusions

We assessed the effect of two rotational positions of WW on soil bacterial and archaeal abundance and their dynamics by measuring extracellular enzymatic activity, N cycling and yield of WW. Our results highlight the vulnerability of successive WW rotations and the benefit of introducing the N-rich oilseed rape in the rotation. The soil legacy of the preceding crops caused distinct PSFs by shaping the microbial communities and enzymatic activities, which affected N availability for the subsequent growth and yield of WW. The higher grain yield in W1 was due to increased root growth and soil mineral N during its early growth phase. Conversely, W2 exhibited distinct responses to the lower initial soil N as observed by the higher abundances of N-fixing genes, nitrification and denitrification-related genes, which were unable to compensate for this early N limitation, resulting in substantial yield losses. This study improves our mechanistic understanding of how the preceding crops influence key rhizosphere processes that create unique soil legacies for the following WW.

CRediT authorship contribution statement

Nikolaos Kaloterakis: Writing – review & editing, Writing – original draft, Visualization, Validation, Software, Methodology, Investigation, Funding acquisition, Formal analysis, Data curation, Conceptualization. Adriana Giongo: Writing – review & editing, Writing – original draft, Visualization, Validation, Software, Methodology, Data curation. Andrea Braun-Kiewnick: Writing – review & editing, Visualization, Methodology, Mehdi Rashtbari: Writing – review & editing, Visualization, Methodology, Data curation. Priscilla Zamberlan: Writing – review & editing, Visualization, Software, Methodology, Data curation. Bahar S. Razavi: Writing – review & editing, Project administration, Methodology. Kornelia Smalla: Writing – review & editing, Project administration, Methodology. Rüdiger Reichel: Writing – review & editing. Nicolas Brüggemann: Writing – review & editing, Supervision, Resources, Project administration, Investigation, Funding acquisition, Conceptualization.

Data availability

The data will be uploaded to the BonaRes Repository for Soil and Agricultural Research Data. Raw amplicon data were deposited in the National Center for Biotechnology Information (NCBI) Sequence Read Archive (SRA) under BioProject PRJNA942109.

Declaration of generative AI and AI-assisted technologies in the writing process

During the preparation of this work the author(s) used "Language-Tool Your writing assistant (Language-Tooler GmbH, Potsdam, Germany)" to improve the grammar of the text. After using this tool/service, the author(s) reviewed and edited the content as needed and take(s) full responsibility for the content of the publication.

Funding

This work was conducted within the RhizoWheat Project, project number 031B0910A (CAU), 031B0910B (Forschungszentrum Jülich), and 031B0910D (Julius Kühn Institute), funded by the Federal Ministry of Education and Research (BMBF) under the Funding Program "Rhizo4Bio - Importance of the Rhizosphere for the Bioeconomy". AG was funded through the 2018–2019 BiodivERsA3 ERA-Net COFUND program, and by the German Research Foundation (DFG, grant number SM 59/21–1).

Declaration of competing interest

The authors declare that they have no known competing financial interests or personal relationships that could have appeared to influence the work reported in this paper.

Acknowledgments

The authors acknowledge Henning Kage, Nora Honsdorf and Katharina Pronkow (Christian-Albrechts-University of Kiel, CAU) for providing the soil and seed material for the experiment. We also acknowledge the support of Charlotte Kummer and Katarina Kuusk in root scanning and soil sampling, respectively. We extend our gratitude to Prof. Dr. Christoph Tebbe from the Thünen Institute (Braunschweig, Germany) and Prof. Dr. Michael Schloter from the Helmholtz Zentrum München (Germany) for generously providing the reference DNA used as qPCR standards. Finally, we acknowledge the assistance of Holger Wissel in the soil and plant C and N analyses.

Appendix A. Supplementary data

Supplementary data to this article can be found online at $\frac{\text{https:}}{\text{doi.}}$ org/10.1016/j.soilbio.2025.109729.

References

- Adesina, M.F., Lembke, A., Costa, R., Speksnijder, A., Smalla, K., 2007. Screening of bacterial isolates from various European soils for in vitro antagonistic activity towards Rhizoctonia solani and Fusarium oxysporum: site-dependent composition and diversity revealed. Soil Biology and Biochemistry 39, 2818–2828. https://doi. org/10.1016/j.soilbio.2007.06.004.
- Alegria Terrazas, R., Robertson-Albertyn, S., Corral, A.M., Escudero-Martinez, C., Kapadia, R., Balbirnie-Cumming, K., Morris, J., Hedley, P.E., Barret, M., Torres-Cortes, G., Paterson, E., Baggs, E.M., Abbott, J., Bulgarelli, D., 2022. Defining composition and function of the rhizosphere microbiota of barley genotypes exposed to growth-limiting nitrogen supplies. mSystems 7, e00934. https://doi.org/10.1128/ msystems.00934-22, 22.
- Alves, R.J.E., Minh, B.Q., Urich, T., von Haeseler, A., Schleper, C., 2018. Unifying the global phylogeny and environmental distribution of ammonia-oxidising archaea based on amoA genes. Nature Communications 9, 1517. https://doi.org/10.1038/ s41467-018-03861-1.
- Angus, J.F., Kirkegaard, J.A., Hunt, J.R., Ryan, M.H., Ohlander, L., Peoples, M.B., 2015.
 Break crops and rotations for wheat. Crop & Pasture Science 66, 523–552. https://doi.org/10.1071/CP14252
- Arnhold, J., Grunwald, D., Braun-Kiewnick, A., Koch, H.-J., 2023a. Effect of crop rotational position and nitrogen supply on root development and yield formation of winter wheat. Frontiers in Plant Science 14. https://doi.org/10.3389/fpls.2023.1265994.

- Arnhold, J., Grunwald, D., Kage, H., Koch, H.-J., 2023b. No differences in soil structure under winter wheat grown in different crop rotational positions. Canadian Journal of Soil Science 103, 643–649. https://doi.org/10.1139/cjss-2023-0030.
- Bacilio-Jiménez, M., Aguilar-Flores, S., del Valle, M., Pérez, A., Zepeda, A., Zenteno, E., 2001. Endophytic bacteria in rice seeds inhibit early colonization of roots by Azospirillum brasilense. Soil Biology and Biochemistry 33, 167–172. https://doi. org/10.1016/S0038-0717(00)00126-7.
- Banerjee, S., Kirkby, C.A., Schmutter, D., Bissett, A., Kirkegaard, J.A., Richardson, A.E., 2016. Network analysis reveals functional redundancy and keystone taxa amongst bacterial and fungal communities during organic matter decomposition in an arable soil. Soil Biology and Biochemistry 97, 188–198. https://doi.org/10.1016/j. soilbio.2016.03.017.
- Benizri, E., Nguyen, C., Piutti, S., Slezack-Deschaumes, S., Philippot, L., 2007. Additions of maize root mucilage to soil changed the structure of the bacterial community. Soil Biology and Biochemistry 39, 1230–1233. https://doi.org/10.1016/j. soilbio.2006.12.026
- Braun-Kiewnick, A., Giongo, A., Zamberlan, P.M., Pluta, P., Koch, H.-J., Kage, H., Smalla, K., Babin, D., 2024. The microbiome of continuous wheat rotations: minor shifts in bacterial and archaeal communities but a source for functionally active plant-beneficial bacteria. Phytobiomes Journal. https://doi.org/10.1094/PBIOMES-05-24-0054-R
- Callahan, B.J., McMurdie, P.J., Rosen, M.J., Han, A.W., Johnson, A.J.A., Holmes, S.P., 2016. DADA2: high-resolution sample inference from Illumina amplicon data. Nature Methods 13, 581–583. https://doi.org/10.1038/nmeth.3869.
- Caporaso, J.G., Lauber, C.L., Walters, W.A., Berg-Lyons, D., Lozupone, C.A., Turnbaugh, P.J., Fierer, N., Knight, R., 2011. Global patterns of 16S rRNA diversity at a depth of millions of sequences per sample. Proceedings of the National Academy of Sciences of the United States of America 108, 4516–4522. https://doi.org/ 10.1073/pnas.1000080107.
- Cerecetto, V., Leoni, C., Jurburg, S.D., Kampouris, I.D., Smalla, K., Babin, D., 2024. Pasture-crop rotations modulate the soil and rhizosphere microbiota and preserve soil structure supporting oat cultivation in the Pampa biome. Soil Biology and Biochemistry 195, 109451. https://doi.org/10.1016/j.soilbio.2024.109451.
- Chen, D., Wang, X., Carrión, V.J., Yin, S., Yue, Z., Liao, Y., Dong, Y., Li, X., 2022. Acidic amelioration of soil amendments improves soil health by impacting rhizosphere microbial assemblies. Soil Biology and Biochemistry 167, 108599. https://doi.org/ 10.1016/j.soilbio.2022.108599.
- Chen, Q., Long, C., Bao, Y., Men, X., Zhang, Y., Cheng, X., 2024. The dominant genera of nitrogenase (nifH) affects soil biological nitrogen fixation along an elevational gradient in the Hengduan mountains. Chemosphere 347, 140722. https://doi.org/ 10.1016/i.chemosphere.2023.140722.
- Chen, Y., Li, Y., Qiu, T., He, H., Liu, J., Duan, C., Cui, Y., Huang, M., Wu, C., Fang, L., 2023. High nitrogen fertilizer input enhanced the microbial network complexity in the paddy soil. Soil Ecology Letters 6, 230205. https://doi.org/10.1007/s42832-023-0205-3
- Contosta, A.R., Frey, S.D., Cooper, A.B., 2011. Seasonal dynamics of soil respiration and N mineralization in chronically warmed and fertilized soils. Ecosphere 2, art36. https://doi.org/10.1890/ES10-00133.1.
- D'Acunto, L., Andrade, J.F., Poggio, S.L., Semmartin, M., 2018. Diversifying crop rotation increased metabolic soil diversity and activity of the microbial community. Agriculture, Ecosystems & Environment 257, 159–164. https://doi.org/10.1016/j. agee.2018.02.011.
- Daims, H., Lebedeva, E.V., Pjevac, P., Han, P., Herbold, C., Albertsen, M., Jehmlich, N., Palatinszky, M., Vierheilig, J., Bulaev, A., Kirkegaard, R.H., von Bergen, M., Rattei, T., Bendinger, B., Nielsen, P.H., Wagner, M., 2015. Complete nitrification by Nitrospira bacteria. Nature 528, 504–509. https://doi.org/10.1038/nature16461.
- Erenstein, O., Jaleta, M., Mottaleb, K.A., Sonder, K., Donovan, J., Braun, H.-J., 2022.
 Global trends in wheat production, consumption and trade BT wheat improvement.
 In: Reynolds, M.P., Braun, H.-J. (Eds.), Food Security in a Changing Climate.
 Springer International Publishing, Cham, pp. 47–66. https://doi.org/10.1007/978-30.30.00673.3
- Gao, Z., Han, M., Hu, Y., Li, Z., Liu, C., Wang, X., Tian, Q., Jiao, W., Hu, J., Liu, L., Guan, Z., Ma, Z., 2019. Effects of continuous cropping of sweet potato on the fungal community structure in rhizospheric soil. Frontiers in Microbiology 10, 2269. https://doi.org/10.3389/fmicb.2019.02269.
- George, T.S., Bulgarelli, D., Carminati, A., Chen, Y., Jones, D., Kuzyakov, Y., Schnepf, A., Wissuwa, M., Roose, T., 2024. Bottom-up perspective the role of roots and rhizosphere in climate change adaptation and mitigation in agroecosystems. Plant and Soil 500, 297–323. https://doi.org/10.1007/s11104-024-06626-6.
- German, D.P., Chacon, S.S., Allison, S.D., 2011. Substrate concentration and enzyme allocation can affect rates of microbial decomposition. Ecology 92, 1471–1480. https://doi.org/10.1890/10-2028.1.
- Giongo, A., Arnhold, J., Grunwald, D., Smalla, K., Braun-Kiewnick, A., 2024. Soil depths and microhabitats shape soil and root-associated bacterial and archaeal communities more than crop rotation in wheat. Frontiers in Microbiomes 3, 1–14. https://doi.org/ 10.3389/frmbj. 2024. 1335701
- Groeneveld, M., Grunwald, D., Piepho, H.P., Koch, H.J., 2024. Crop rotation and sowing date effects on yield of winter wheat. Journal of Agricultural Science 162, 139–149. https://doi.org/10.1017/S0021859624000261.
- Hansen, J.C., Schillinger, W.F., Sullivan, T.S., Paulitz, T.C., 2019. Soil microbial biomass and fungi reduced with canola introduced into long-term monoculture wheat rotations. Frontiers in Microbiology 10, 1488. https://doi.org/10.3389/ fmicb.2019.01488.
- Hao, J., Feng, Y., Wang, Xing, Yu, Q., Zhang, F., Yang, G., Ren, G., Han, X., Wang, Xiaojiao, Ren, C., 2022. Soil microbial nitrogen-cycling gene abundances in

- response to crop diversification: a meta-analysis. Science of the Total Environment 838, 156621. https://doi.org/10.1016/j.scitotenv.2022.156621.
- Hegewald, H., Wensch-Dorendorf, M., Sieling, K., Christen, O., 2018. Impacts of break crops and crop rotations on oilseed rape productivity: a review. European Journal of Agronomy 101, 63–77. https://doi.org/10.1016/j.eja.2018.08.003.
- Henry, S., Bru, D., Stres, B., Hallet, S., Philippot, L., 2006. Quantitative detection of the nosZ gene, encoding nitrous oxide reductase, and comparison of the abundances of 16S rRNA, narG, nirK, and nosZ genes in soils. Applied and Environmental Microbiology 72, 5181–5189. https://doi.org/10.1128/AEM.00231-06.
- Hu, L., Robert, C.A.M.M., Cadot, S., Zhang, X., Ye, M., Li, B., Manzo, D., Chervet, N., Steinger, T., van der Heijden, M.G.A.A., Schlaeppi, K., Erb, M., 2018. Root exudate metabolites drive plant-soil feedbacks on growth and defense by shaping the rhizosphere microbiota. Nature Communications 9, 2738. https://doi.org/10.1038/ s41467-018-05122-7.
- Imparato, V., Hansen, V., Santos, S.S., Nielsen, T.K., Giagnoni, L., Hauggaard-Nielsen, H., Johansen, A., Renella, G., Winding, A., 2016. Gasification biochar has limited effects on functional and structural diversity of soil microbial communities in a temperate agroecosystem. Soil Biology and Biochemistry 99, 128–136. https://doi.org/ 10.1016/j.soilbio.2016.05.004.
- Jeewani, P.H., Luo, Y., Yu, G., Fu, Y., He, X., Van Zwieten, L., Liang, C., Kumar, A., He, Y., Kuzyakov, Y., Qin, H., Guggenberger, G., Xu, J., 2021. Arbuscular mycorrhizal fungi and goethite promote carbon sequestration via hyphal-aggregate mineral interactions. Soil Biology and Biochemistry 162, 108417. https://doi.org/ 10.1016/j.soilbio.2021.108417.
- Kaloterakis, N., Kummer, S., Le Gall, S., Rothfuss, Y., Reichel, R., Brüggemann, N., 2024a. Reduced belowground allocation of freshly assimilated C contributes to negative plant-soil feedback in successive winter wheat rotations. Plant and Soil. https://doi.org/10.1007/s11104-024-06696-6.
- Kaloterakis, N., Rashtbari, M., Razavi, B.S., Braun-Kiewnick, A., Giongo, A., Smalla, K., Kummer, C., Kummer, S., Reichel, R., Brüggemann, N., 2024b. Preceding crop legacy modulates the early growth of winter wheat by influencing root growth dynamics, rhizosphere processes, and microbial interactions. Soil Biology and Biochemistry 191, 109343, https://doi.org/10.1016/j.soilbio.2024.109343.
- Kerdraon, L., Balesdent, M.-H., Barret, M., Laval, V., Suffert, F., 2019. Crop residues in wheat-oilseed rape rotation system: a pivotal, shifting platform for microbial meetings. Microbial Ecology 77, 931–945. https://doi.org/10.1007/s00248-019-01340-8
- Koprivova, A., Kopriva, S., 2022. Plant secondary metabolites altering root microbiome composition and function. Current Opinion in Plant Biology 67, 102227. https://doi. org/10.1016/j.pbi.2022.102227.
- Lahti, L., Shetty, S., 2017. microbiome: tools for microbiome analysis in R. Available at: https://github.com/microbiome/microbiome/.
- Leininger, S., Urich, T., Schloter, M., Schwark, L., Qi, J., Nicol, G.W., Prosser, J.I., Schuster, S.C., Schleper, C., 2006. Archaea predominate among ammonia-oxidizing prokaryotes in soils. Nature 442, 806–809. https://doi.org/10.1038/nature04983.
- Levičnik-Höfferle, Š., Nicol, G.W., Ausec, L., Mandić-Mulec, I., Prosser, J.I., 2012.
 Stimulation of thaumarchaeal ammonia oxidation by ammonia derived from organic nitrogen but not added inorganic nitrogen. FEMS Microbiology Ecology 80, 114-123. https://doi.org/10.1111/j.1574-6941.2011.01275.x
- 114–123. https://doi.org/10.1111/j.1574-6941.2011.01275.x.
 Ling, N., Wang, T., Kuzyakov, Y., 2022. Rhizosphere bacteriome structure and functions.
 Nature Communications 13, 836. https://doi.org/10.1038/s41467-022-28448-9.
- Liu, H., Colombi, T., Jäck, O., Westerbergh, A., Weih, M., 2022. Linking wheat nitrogen use to root traits: shallow and thin embryonic roots enhance uptake but reduce conversion efficiency of nitrogen. Field Crops Research 285, 108603. https://doi. org/10.1016/i.fcr.2022.108603.
- Liu, R., Liu, Y., Gao, Y., Zhao, F., Wang, J., 2023. The nitrogen cycling key functional genes and related microbial bacterial community α –Diversity is determined by crop rotation plans in the loess plateau. Agronomy. https://doi.org/10.3390/agronomy13071769.
- Love, M.I., Huber, W., Anders, S., 2014. Moderated estimation of fold change and dispersion for RNA-seq data with DESeq2. Genome Biology 15, 550. https://doi.org/ 10.1186/s13059-014-0550-8.
- Maheshwari, A., Jones, C.M., Tiemann, M., Hallin, S., 2023. Carbon substrate selects for different lineages of N2O reducing communities in soils under anoxic conditions. Soil Biology and Biochemistry 177, 108909. https://doi.org/10.1016/j. soilbio.2022.108909.
- McMurdie, P.J., Holmes, S., 2013. Phyloseq: an R package for reproducible interactive analysis and graphics of microbiome census data. PLoS One 8, e61217. https://doi. org/10.1371/journal.pone.0061217.
- Meyer, A., Focks, A., Radl, V., Keil, D., Welzl, G., Schöning, I., Boch, S., Marhan, S., Kandeler, E., Schloter, M., 2013. Different land use intensities in grassland ecosystems drive ecology of microbial communities involved in nitrogen turnover in soil. PLoS One 8, e73536. https://doi.org/10.1371/journal.pone.0073536.
- Moore, F.C., Lobell, D.B., 2015. The fingerprint of climate trends on european crop yields. Proceedings of the National Academy of Sciences of the United States of America 112, 2970–2975. https://doi.org/10.1073/pnas.1409606112.
- Mwendwa, J.M., Weston, P.A., Weidenhamer, J.D., Fomsgaard, I.S., Wu, H., Gurusinghe, S., Weston, L.A., 2021. Metabolic profiling of benzoxazinoids in the roots and rhizosphere of commercial winter wheat genotypes. Plant and Soil 466, 467–489. https://doi.org/10.1007/s11104-021-04996-9.
- Navarro-Noya, Y.E., Gómez-Acata, S., Montoya-Ciriaco, N., Rojas-Valdez, A., Suárez-Arriaga, M.C., Valenzuela-Encinas, C., Jiménez-Bueno, N., Verhulst, N., Govaerts, B., Dendooven, L., 2013. Relative impacts of tillage, residue management and croprotation on soil bacterial communities in a semi-arid agroecosystem. Soil Biology and Biochemistry 65, 86–95. https://doi.org/10.1016/j.soilbio.2013.05.009.

- Oksanen, J., Simpson, G.L., Blanchet, F.G., Kindt, R., Legendre, P., Minchin, P.R., O'Hara, R.B., Solymos, P., Stevens, M.H.H., Szoecs, E., Wagner, H., Barbour, M., Bedward, M., Bolker, B., Borcard, D., Carvalho, G., Chirico, M., De Caceres, M., Durand, S., Evangelista, H.B.A., FitzJohn, R., Friendly, M., Furneaux, B., Hannigan, G., Hill, M.O., Lahti, L., McGlinn, D., Ouellette, M.-H., Ribeiro Cunha, E., Smith, T., Stier, A., Ter Braak, C.J.F., Weedon, J., 2022. Vegan: community ecology package. R Package Version 2, 6–8. https://doi.org/10.32614/CRAN.package.vegan.
- Palma-Guerrero, J., Chancellor, T., Spong, J., Canning, G., Hammond, J., McMillan, V.E., Hammond-Kosack, K.E., 2021. Take-all disease: new insights into an important wheat root pathogen. Trends in Plant Science 26, 836–848. https://doi.org/ 10.1016/j.tplants.2021.02.009.
- Patil, I., 2021. Visualizations with statistical details: the 'ggstatsplot' approach. Journal of Open Source Software 6, 1–5. https://doi.org/10.21105/joss.03167.
- Poly, F., Ranjard, L., Nazaret, S., Gourbière, F., Monrozier, L.J., 2001. Comparison of nifH gene pools in soils and soil microenvironments with contrasting properties. Applied and Environmental Microbiology 67, 2255–2262. https://doi.org/10.1128/ AEM.67.5.2255-2262.2001.
- Quast, C., Pruesse, E., Yilmaz, P., Gerken, J., Schweer, T., Yarza, P., Peplies, J., Glöckner, F.O., 2013. The SILVA ribosomal RNA gene database project: improved data processing and web-based tools. Nucleic Acids Research 41, 590–596. https:// doi.org/10.1093/nar/gks1219.
- R Core Team, 2022. R: a Language and Environment for Statistical Computing. R Foundation for Statistical Computing, Vienna, Austria. http://www.r-project.org.
- Razavi, B.S., Liu, S., Kuzyakov, Y., 2017. Hot experience for cold-adapted microorganisms: temperature sensitivity of soil enzymes. Soil Biology and Biochemistry 105, 236–243. https://doi.org/10.1016/j.soilbio.2016.11.026.
- Reichel, R., Kamau, C.W., Kumar, A., Li, Z., Radl, V., Temperton, V.M., Schloter, M., Brüggemann, N., 2022. Spring barley performance benefits from simultaneous shallow straw incorporation and top dressing as revealed by rhizotrons with resealable sampling ports. Biology and Fertility of Soils 58, 375–388. https://doi. org/10.1007/s00374-022-01624-1.
- Rotthauwe, J.H., Witzel, K.P., Liesack, W., 1997. The ammonia monooxygenase structural gene amoA as a functional marker: molecular fine-scale analysis of natural ammonia-oxidizing populations. Applied and Environmental Microbiology 63, 4704–4712. https://doi.org/10.1128/aem.63.12.4704-4712.1997.
- Sakai, K., Yamauchi, N., Tatsuo, F., Ohe, T., 1996. Biodegradation of cellulose acetate by Neisseria sicca. Bioscience, Biotechnology, and Biochemistry 60, 1617–1622. https://doi.org/10.1271/bbb.60.1617.
- Santana, M.M., Dias, T., Gonzalez, J.M., Cruz, C., 2021. Transformation of organic and inorganic sulfur– adding perspectives to new players in soil and rhizosphere. Soil Biology and Biochemistry 160, 108306. https://doi.org/10.1016/j. soilbio.2021.108306.
- Santana, M.M., Portillo, M.C., Gonzalez, J.M., Clara, M.I.E., 2013. Characterization of new soil thermophilic bacteria potentially involved in soil fertilization. Journal of Plant Nutrition and Soil Science 176, 47–56. https://doi.org/10.1002/ ipln.201100382.
- Sasse, J., Martinoia, E., Northen, T., 2018. Feed Your friends: do plant exudates shape the root microbiome? Trends in Plant Science 23, 25–41. https://doi.org/10.1016/j. tplants.2017.09.003.
- Schauberger, B., Ben-Ari, T., Makowski, D., Kato, T., Kato, H., Ciais, P., 2018. Yield trends, variability and stagnation analysis of major crops in France over more than a century. Scientific Reports 8, 16865. https://doi.org/10.1038/s41598-018-35351-1.
- Schauss, K., Focks, A., Leininger, S., Kotzerke, A., Heuer, H., Thiele-Bruhn, S., Sharma, S., Wilke, B.-M., Matthies, M., Smalla, K., Munch, J.C., Amelung, W., Kaupenjohann, M., Schloter, M., Schleper, C., 2009. Dynamics and functional relevance of ammonia-oxidizing archaea in two agricultural soils. Environmental Microbiology 11, 446–456. https://doi.org/10.1111/j.1462-2920.2008.01783.x.
- Schloss, P.D., 2024. Rarefaction is currently the best approach to control for uneven sequencing effort in amplicon sequence analyses. mSphere 9, e00354. https://doi. org/10.1128/msphere.00354-23, 23.
- Shewry, P.R., Hey, S.J., 2015. The contribution of wheat to human diet and health. Food and Energy Security 4, 178–202. https://doi.org/10.1002/FES3.64.
- Sieling, K., Stahl, C., Winkelmann, C., Christen, O., 2005. Growth and yield of winter wheat in the first 3 years of a monoculture under varying N fertilization in NW Germany. European Journal of Agronomy 22, 71–84. https://doi.org/10.1016/j. eja.2003.12.004.
- Simonet, P., Grosjean, M.C., Misra, A.K., Nazaret, S., Cournoyer, B., Normand, P., 1991. Frankia genus-specific characterization by polymerase chain reaction. Applied and Environmental Microbiology 57, 3278–3286. https://doi.org/10.1128/ aem.57.11.3278-3286.1991.
- Sterngren, A.E., Hallin, S., Bengtson, P., 2015. Archaeal ammonia oxidizers dominate in numbers, but bacteria drive gross nitrification in N-amended grassland soil. Frontiers in Microbiology 6, 1350. https://doi.org/10.3389/fmicb.2015.01350.
- Sun, L., Wang, S., Narsing Rao, M.P., Shi, Y., Lian, Z.-H., Jin, P.-J., Wang, W., Li, Y.-M., Wang, K.-K., Banerjee, A., Cui, X.-Y., Wei, D., 2023. The shift of soil microbial community induced by cropping sequence affect soil properties and crop yield. Frontiers in Microbiology 14. https://doi.org/10.3389/fmicb.2023.1095688.
- Sundberg, C., Al-Soud, W.A., Larsson, M., Alm, E., Yekta, S.S., Svensson, B.H., Sørensen, S.J., Karlsson, A., 2013. 454 pyrosequencing analyses of bacterial and archaeal richness in 21 full-scale biogas digesters. FEMS Microbiology Ecology 85, 612–626. https://doi.org/10.1111/1574-6941.12148.
- Suzuki, M.T., Taylor, L.T., DeLong, E.F., 2000. Quantitative analysis of small-subunit rRNA genes in mixed microbial populations via 5'-nuclease assays. Applied and

- Environmental Microbiology 66, 4605–4614. https://doi.org/10.1128/AEM.66.11.4605-4614.2000.
- Throbäck, I.N., Enwall, K., Jarvis, A., Hallin, S., 2004. Reassessing PCR primers targeting nirS, nirK and nosZ genes for community surveys of denitrifying bacteria with DGGE. FEMS Microbiology Ecology 49, 401–417. https://doi.org/10.1016/j. femsec.2004.04.011.
- Town, J.R., Dumonceaux, T., Tidemann, B., Helgason, B.L., 2023. Crop rotation significantly influences the composition of soil, rhizosphere, and root microbiota in canola (Brassica napus L.). Environmental Microbiome 18, 1–14. https://doi.org/ 10.1186/s40793-023-00495-9.
- Wang, Y., Zhang, Y., Li, Z.-Z., Zhao, Q., Huang, X.-Y., Huang, K.-F., 2019. Effect of continuous cropping on the rhizosphere soil and growth of common buckwheat. Plant Production Science 23, 81–90. https://doi.org/10.1080/1343943X.2019.1685895.
- Wassermann, B., Cernava, T., Goertz, S., Zur, J., Rietz, S., Kögl, I., Abbadi, A., Berg, G., 2023. Low nitrogen fertilization enriches nitrogen-fixing bacteria in the Brassica seed microbiome of subsequent generations. Journal of Sustainable Agriculture and Environment 2, 87–98. https://doi.org/10.1002/sae2.12046.
- Wei, W., Isobe, K., Nishizawa, T., Zhu, L., Shiratori, Y., Ohte, N., Koba, K., Otsuka, S., Senoo, K., 2015. Higher diversity and abundance of denitrifying microorganisms in environments than considered previously. The ISME Journal 9, 1954–1965. https:// doi.org/10.1038/ismej.2015.9.
- Weiser, C., Fuß, R., Kage, H., Flessa, H., 2017. Do farmers in Germany exploit the potential yield and nitrogen benefits from preceding oilseed rape in winter wheat cultivation? Archives of Agronomy and Soil Science 64, 25–37. https://doi.org/ 10.1080/03650340.2017.1326031.
- Wemheuer, F., Taylor, J.A., Daniel, R., Johnston, E., Meinicke, P., Thomas, T., Wemheuer, B., 2020. Tax4Fun2: prediction of habitat-specific functional profiles and functional redundancy based on 16S rRNA gene sequences. Environmental Microbiome 15, 11. https://doi.org/10.1186/s40793-020-00358-7.
- Wickham, H., 2016. ggplot2: Elegant Graphics for Data Analysis. Springer-Verlag, New York.
- Wolińska, A., Kuźniar, A., Zielenkiewicz, U., Banach, A., Izak, D., Stępniewska, Z., Błaszczyk, M., 2017. Metagenomic analysis of some potential nitrogen-fixing bacteria in arable soils at different formation processes. Microbial Ecology 73, 162–176. https://doi.org/10.1007/s00248-016-0837-2.
- Yang, X., Wang, B., Fakher, A., An, S., Kuzyakov, Y., 2023. Contribution of roots to soil organic carbon: from growth to decomposition experiment. Catena 231, 107317. https://doi.org/10.1016/j.catena.2023.107317.
- Yang, Y., Liu, H., Lv, J., 2022. Response of N2O emission and denitrification genes to different inorganic and organic amendments. Scientific Reports 12, 3940. https:// doi.org/10.1038/s41598-022-07753-9.
- Yeo, I.N.K., Johnson, R.A., 2000. A new family of power transformations to improve normality or symmetry. Biometrika 87, 954–959. https://doi.org/10.1093/biomet/ 87.4.954.
- Yin, C., Schlatter, D.C., Hagerty, C.H., Hulbert, S.H., Paulitz, T.C., 2022. Disease-induced assemblage of the rhizosphere fungal community in successive plantings of wheat. Phytobiomes Journal 7, 100–112. https://doi.org/10.1094/pbiomes-12-22-0101-r.
- Yu, P., He, X., Baer, M., Beirinckx, S., Tian, T., Moya, Y.A.T., Zhang, X., Deichmann, M., Frey, F.P., Bresgen, V., Li, C., Razavi, B.S., Schaaf, G., von Wirén, N., Su, Z., Bucher, M., Tsuda, K., Goormachtig, S., Chen, X., Hochholdinger, F., 2021. Plant flavones enrich rhizosphere Oxalobacteraceae to improve maize performance under nitrogen deprivation. Nature Plants 7, 481–499. https://doi.org/10.1038/s41477-021-00897-v.
- Yu, T., Hou, X., Fang, X., Razavi, B., Zang, H., Zeng, Z., Yang, Y., 2024. Short-term continuous monocropping reduces peanut yield mainly via altering soil enzyme activity and fungal community. Environmental Research 245, 117977. https://doi. org/10.1016/j.envres.2023.117977.
- Yu, Y., Lee, C., Kim, J., Hwang, S., 2005. Group-specific primer and probe sets to detect methanogenic communities using quantitative real-time polymerase chain reaction. Biotechnology and Bioengineering 89, 670–679. https://doi.org/10.1002/
- Yuan, J., Zhao, J., Wen, T., Zhao, M., Li, R., Goossens, P., Huang, Q., Bai, Y., Vivanco, J. M., Kowalchuk, G.A., Berendsen, R.L., Shen, Q., 2018. Root exudates drive the soil-borne legacy of aboveground pathogen infection. Microbiome 6, 156. https://doi.org/10.1186/s40168-018-0537-x.
- Zadoks, J.C., Chang, T.T., Konzak, C.F., 1974. A decimal code for the growth stages of cereals. Weed Research 14, 415–421. https://doi.org/10.1111/j.1365-3180.1974. tb01084.x.
- Zheng, J., Fujii, K., Koba, K., Wanek, W., Müller, C., Jansen-Willems, A.B., Nakajima, Y., Wagai, R., Canarini, A., 2023. Revisiting process-based simulations of soil nitrite dynamics: tighter cycling between nitrite and nitrate than considered previously. Soil Biology and Biochemistry 178, 108958. https://doi.org/10.1016/j.soilbio.2023.108958
- Zhou, Y., Yang, Z., Liu, J., Li, Xudong, Wang, X., Dai, C., Zhang, T., Carrión, V.J., Wei, Z., Cao, F., Delgado-Baquerizo, M., Li, Xiaogang, 2023. Crop rotation and native microbiome inoculation restore soil capacity to suppress a root disease. Nature Communications 14, 8126. https://doi.org/10.1038/s41467-023-43926-4.
- Zumft, W.G., 1997. Cell biology and molecular basis of denitrification. Microbiology and Molecular Biology Reviews 61, 533-616. https://doi.org/10.1128/mmbr.61.4.533-616.1007